

Quantitative Measurement of the $\nu = \frac{5}{2}$ Fractional Quantum Hall State Gap

by

William Scales

A THESIS SUBMITTED IN PARTIAL FULFILLMENT
OF THE REQUIREMENTS FOR THE DEGREE OF

Bachelor of Science

in

THE FACULTY OF SCIENCE

(Physics and Astronomy)

The University Of British Columbia
(Vancouver)

April 2013

© William Scales, 2013

Abstract

The fractional quantum Hall effect (FQHE) is a novel state of matter which is observed in strongly correlated two-dimensional electron systems. In this thesis, we investigate the activation gap of the $\nu = \frac{5}{2}$ FQHE state by thermal activation methods. This state, not explained by the existing composite fermion theory, is conjectured to support quasiparticle excitations which obey fractional statistics—in-between Bose and Fermi statistics. The $\frac{5}{2}$ state is a promising candidate for topologically protected quantum computing. Measurements of its activation gap can confirm some aspects of its suitability for quantum computing and help to develop fabrication techniques.

Preface

The GaAs-AlGaAs quantum well sample measured in this thesis was provided by Prof. Michael Manfra of Purdue University. Sample preparation was carried out by Alexandr Rossokhaty. Some of the data used in the analysis were measured by Mohammad Samani. Literature review, experiment design, data collection, data analysis, and manuscript preparation were done by William Scales under the supervision of Joshua Folk.

Table of Contents

| | |
|--------------------------------------|-------------|
| Abstract | ii |
| Preface | iii |
| Table of Contents | iv |
| List of Figures | vi |
| List of Symbols | viii |
| List of Abbreviations | ix |
| Acknowledgements | x |
| 1 Introduction | 1 |
| 2 Theory | 5 |
| 2.1 Classical Hall Effect | 5 |
| 2.2 Two-Dimensional Electron Systems | 6 |
| 2.3 Integral Quantum Hall Effect | 7 |
| 2.3.1 Landau Levels | 7 |
| 2.3.2 Localization | 8 |
| 2.3.3 Edge States | 10 |
| 2.4 Fractional Quantum Hall Effect | 11 |
| 2.4.1 The $\frac{5}{2}$ State | 12 |
| 2.4.2 Thermal Activation | 12 |
| 3 Experiment | 13 |
| 3.1 Sample | 13 |
| 3.2 Measurement | 13 |
| 4 Results and Discussion | 15 |

| | |
|-------------------------------|-----------|
| 5 Conclusion | 19 |
| Bibliography | 20 |

List of Figures

| | | |
|------------|--|----|
| Figure 1.1 | The experimental signature of the integral quantum Hall effect (IQHE). | 2 |
| Figure 1.2 | A typical device for quantum Hall transport measurements. This figure depicts the “Hall bar” geometry, where current is injected at one end of a rectangular device and extracted at the other end. R_L is measured parallel to the flow of current while R_H is measured perpendicular to the current. | 3 |
| Figure 1.3 | Longitudinal resistance (R_{xx} or R_L) for a high mobility sample clearly showing many well-developed FQHE states. As in Figure 1.1, each state corresponds to a minimum in R_{xx} | 4 |
| Figure 2.1 | The classical Hall effect. In the laboratory, one measures a transverse voltage V_H and a longitudinal voltage V_L and obtains the resistances by $R_H = V_H/I$ and $R_L = V_L/I$ | 6 |
| Figure 2.2 | Band diagram of a GaAs-AlGaAs quantum well. The difference in band gaps between AlGaAs and GaAs creates a potential well. A two-dimensional electron gas (2DEG) is created when the AlGaAs is doped with electrons. The donors migrate into the GaAs and fall into the potential well, thus becoming confined. The horizontal axis corresponds to the direction of deposition on the physical wafer. . . . | 7 |
| Figure 2.3 | Landau level (LL) density of states (DOS) for clean (left) and dirty (right) samples. | 9 |
| Figure 2.4 | Bending of LLS as a function of transverse position y . Edge channels are formed where the Fermi level intersects upward-bent LLS. | 10 |

| | | |
|------------|--|----|
| Figure 4.1 | Hall and longitudinal resistances for our sample in the filling factor range from $\nu = 2$ to $\nu = 4$. Several well-developed fractional states can be seen along with a number of re-entrant integral states. These are highly interesting in their own right and are due to the formation of crystalline “bubble” and “stripe” phases. These states occur because the electron kinetic energy has frozen out and the electrons seek to minimize their Coulomb energy by forming periodic structures. The measurements shown here were made at base temperature of approximately 12 mK. | 16 |
| Figure 4.2 | Detailed view of the $\frac{5}{2}$ R_L minimum at 12.3 mK. The nonzero value is due to frequency dependent lock-in detection problems that were later fixed. | 17 |
| Figure 4.3 | Thermal activation of the $\frac{5}{2}$ state is clearly evinced as a lifting of the minimum in R_L , which goes from nearly zero resistance to almost $60\ \Omega$ as the temperature of the sample is increased. | 17 |
| Figure 4.4 | Arrhenius plot of thermal activation data. At higher temperatures (corresponding to smaller values of $1/T$), the activation saturates and no longer exhibits an Arrhenius behavior. The two highest temperature points are not included in our fit for this reason. The error bars are one standard deviation. | 18 |

List of Symbols

B applied magnetic field

e elementary charge

h Planck constant

$\hbar\omega_c$ cyclotron energy

n_c density of charge carriers

ν filling factor

R_L, R_{xx}
longitudinal resistance

R_H, R_{xy}
Hall resistance, transverse resistance

ρ_L, ρ_{xx}
longitudinal resistivity

ρ_H, ρ_{xy}
Hall resistivity, transverse resistivity

List of Abbreviations

| | |
|---------------|---|
| 2DEG | two-dimensional electron gas |
| CF | composite fermion |
| DOS | density of states |
| FQHE | fractional quantum Hall effect |
| IQHE | integral quantum Hall effect |
| LL | Landau level |
| MBE | molecular beam epitaxy |
| MOSFET | metal oxide silicon field effect transistor |
| PMMA | poly(methyl methacrylate) |
| QHE | quantum Hall effect |

Acknowledgements

I would like to thank my supervisor, Prof. Joshua Folk, for his endless patience and wisdom in guiding my research. He is an experimental genius who is able to resolve even the most intractable problems. He is always willing to take time away from his busy schedule to provide guidance and advice. Many thanks are also due to Dr. Silvia Leuscher Folk for her invaluable assistance throughout this experiment. Without her help, this thesis never would have been completed.

Alexandr Rossokhaty graciously took time away from his own research to provide me with much essential assistance operating the dilution refrigerator. I am thankful for his willingness to help me troubleshoot fridge problems even at the late hour of 3 am.

Mohammad Samani kindly lent his assistance in carrying out the measurements which underlie this thesis.

Thanks are also due to the others in the Folk lab, each of whom has helped me in some way. Ali Khademi, Mark Lundeborg, and Rui Yang have all assisted me and I am grateful to each of them for their generosity.

Chapter 1

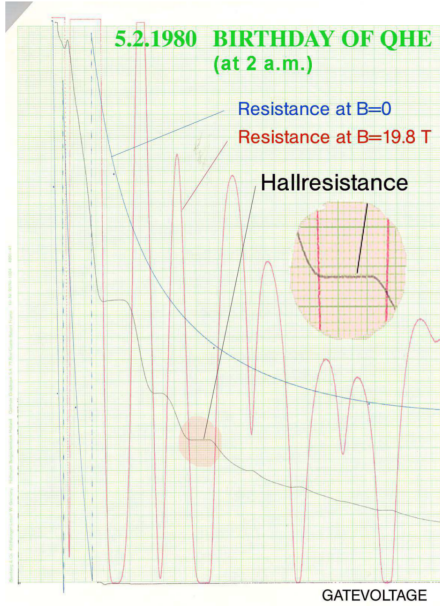
Introduction

One of the most striking and fundamental discoveries in the field of condensed matter in the last thirty years is the 1980 discovery of the integral quantum Hall effect (IQHE) [26] by von Klitzing. Experimentally, the IQHE comprises a dissipationless longitudinal flow of current and an exactly quantized transverse (Hall) resistance

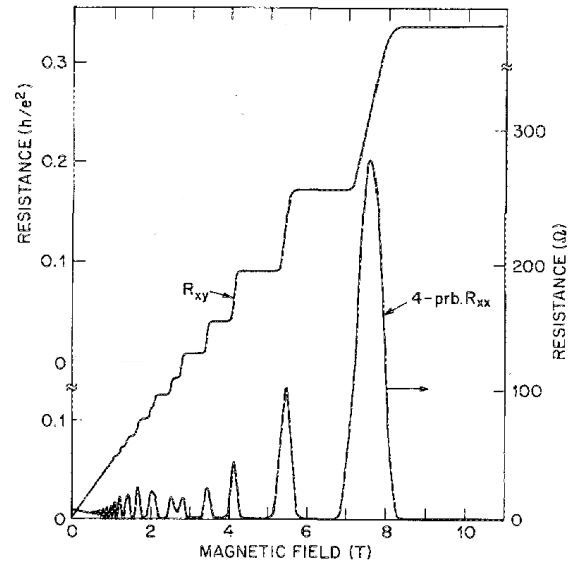
$$R_H = \frac{1}{\nu} \frac{h}{e^2} \quad (1.1)$$

where ν is a quantum number whose values are integers. Physically, ν is equal to the number of filled Landau levels (LLs) (quantized energy states of an electron in a magnetic field), and is called the filling factor. The signature of the IQHE can be seen in Figure 1.1a which depicts von Klitzing’s original experimental trace. Figure 1.1b shows a modern experimental trace exhibiting the IQHE. Moreover, this quantization is exact to within a part in 10^{-9} [19]. This effect is observed at very low temperature in two-dimensional electron systems which are subject, as in the classical Hall effect, to a strong perpendicular magnetic field. Remarkably, the IQHE is essentially independent of device geometry and impurity content. The physics of the IQHE is rooted in the formation of LLs by the two-dimensional electrons and the effects of disorder-induced localization.

More remarkably, in 1982, Tsui, Stormer, and Gossard found that the quantum Hall effect (QHE) could be observed [23] when ν was equal to certain rational fractions—numbers of the form $\frac{p}{q}$ where p and q are both integers. This is called the fractional quantum Hall effect (FQHE). Unlike the IQHE, the FQHE arises due to the strength of electron-electron interactions. In the FQHE, electrons screen the Coulomb interaction by binding to an even number of quantized flux vortices [12] to form “composite



(a) The discovery of the IQHE by K. von Klitzing [25] on February 5, 1980. The trace shows the Hall and longitudinal resistance of a silicon MOSFET at 4.2 K and 19.8 T as a function of the gate voltage. Note that in a MOSFET, increasing the gate voltage increases the carrier density and hence increases the filling factor ν .



(b) A modern IQHE trace, from Pfeiffer [18]. Here, as B increases, the electron density decreases, decreasing the filling factor. Quantized steps in the Hall resistance are clearly seen with corresponding minima in the longitudinal resistance indicating dissipationless transport.

Figure 1.1: The experimental signature of the IQHE.

fermions.” These composite fermions then experience their own IQHE which manifests itself physically as the FQHE. The composite fermion (CF) theory is highly successful and elegant in its simplicity.

CF theory predicts all of the FQHE states which have odd denominators in ν . However, FQHE states have been observed which have even denominators [17, 27, 29], such as $\frac{5}{2}$ and its particle-hole conjugate $\frac{7}{2}$. It is believed that the $\frac{5}{2}$ state is a spin-polarized paired state of composite fermions, analogous to a p-wave BCS state [15]. While the $\frac{5}{2}$ state is not itself a superconducting state, it is incompressible (possesses a nonzero energy gap between the ground state and first excited state). This fact is unexpected and was not predicted by the CF theory. Furthermore, the quasiparticle excitations of the $\frac{5}{2}$ state are conjectured [1, 10] to be “non-Abelian anyons,” obeying non-Abelian braiding statistics. Anyonic statistics form a continuum between Bose statistics and Fermi statistics and particles obeying these statistics have their wave functions multiplied by

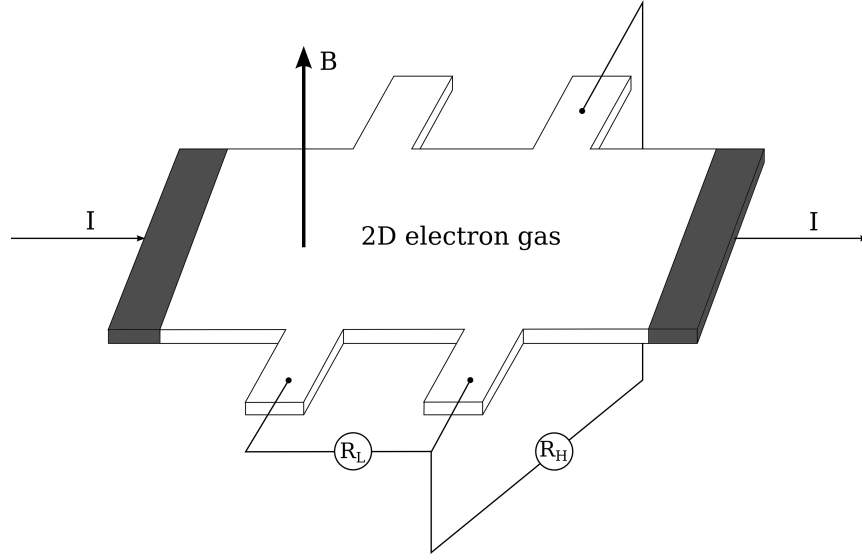


Figure 1.2: A typical device for quantum Hall transport measurements. This figure depicts the “Hall bar” geometry, where current is injected at one end of a rectangular device and extracted at the other end. R_L is measured parallel to the flow of current while R_H is measured perpendicular to the current.

an arbitrary phase factor when exchanged. In the case of non-Abelian anyons, the exchange interaction is not commutative, that is, the precise order in which particles are exchanged matters.

Systems whose excitations are non-Abelian anyons possess multiple degenerate ground states which are “topologically protected.” This means that the ground state is determined solely by the topology of the system and changing between ground states requires braiding of quasiparticle excitations [6]. In other words, the ground state of the system will not evolve into any of the other possible ground states if the temperature is much lower than the excitation gap. This has exciting possibilities for topologically protected quantum computing, in which this property is exploited to limit decoherence of the system and prevent errors [16]. It is believed that the $\frac{5}{2}$ state has the required properties to create topologically protected qubits suitable for quantum computation. Experimental work is underway to confirm that the quasiparticle excitations of the $\frac{5}{2}$ state are indeed non-Abelian anyons [5, 28].

If the $\frac{5}{2}$ state does indeed have multiple, topologically protected ground states, as is believed, then a primary factor in determining its suitability for quantum computing is the size of the excitation gap. It is the incompressibility of the state which provides a buffer against decoherence. The larger the gap, the easier it is to prevent decoherence.

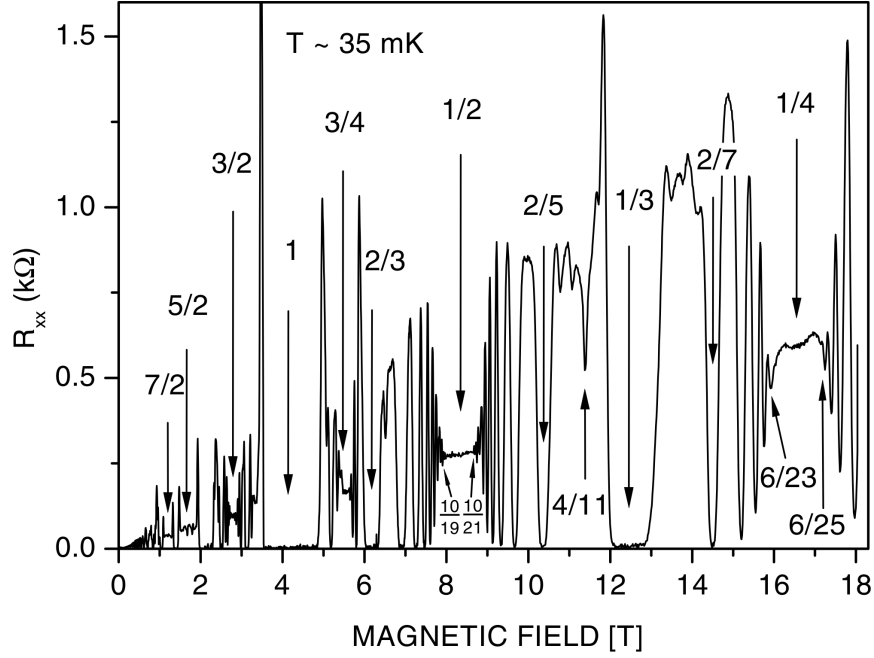


Figure 1.3: Longitudinal resistance (R_{xx} or R_L) for a high mobility sample clearly showing many well-developed FQHE states. As in Figure 1.1, each state corresponds to a minimum in R_{xx} .

Hence, knowing the gap of the $\frac{5}{2}$ state is important in of itself. It is also important to be able to measure the gap to characterize specific experimental samples. Producing experimental samples which exhibit the $\frac{5}{2}$ state is an arduous task and there are many factors which could possibly impact the size of the $\frac{5}{2}$ excitation gap. Thus, a gap measurement provides valuable feedback about the quality of a sample.

In this thesis, we present the results of a measurement of the excitation gap of the $\frac{5}{2}$ state via thermal activation. In Chapter 2, we provide an overview of the theory of the IQHE, FQHE, and the $\frac{5}{2}$ state. We discuss the experimental setup in Chapter 3. Finally, in Chapter 4 we report and discuss our results.

Chapter 2

Theory

2.1 Classical Hall Effect

We will begin by briefly discussing the classical Hall effect so as to better appreciate the profound nature of the QHE. Discovered in 1879 by Edwin Hall [11], the classical Hall effect is the action of a magnetic field on a current flowing in a conductor.

Suppose that a current flows through a rectangular slab of conductor in the \hat{x} direction, as shown in Figure 2.1. This current is composed of moving charge carriers, typically either electrons or holes, each having charge q . Now let the conductor be pierced by a perpendicular magnetic field $\mathbf{B} = B\hat{z}$. In the presence of the magnetic field, the carriers are subject to a Lorentz force

$$\mathbf{F} = q(\mathbf{E} + \mathbf{v} \times \mathbf{B}) \quad (2.1)$$

which causes them to drift in the direction perpendicular to the current with a velocity $\mathbf{v} = (E/B)\hat{y}$. This creates a current density $\mathbf{J} = qn_c\mathbf{v}$, where n_c is the density of carriers. This current density is also directed perpendicular to the original current. Hence, $\mathbf{J} = qn_c(E/B)\hat{y}$. Ohm's law states that locally,

$$\mathbf{E} = \rho\mathbf{J} \quad (2.2)$$

where ρ is the resistivity. Therefore, the classical Hall resistivity is given by

$$\rho_H = \frac{B}{qn_c} \quad (2.3)$$

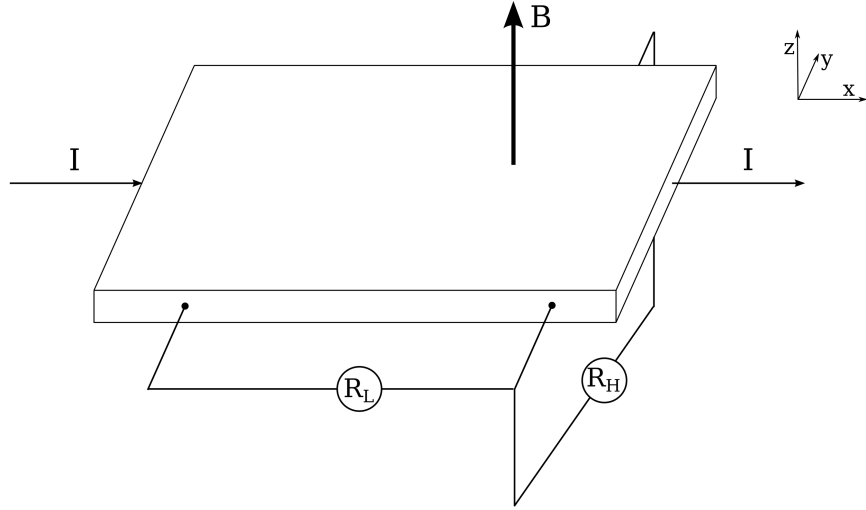


Figure 2.1: The classical Hall effect. In the laboratory, one measures a transverse voltage V_H and a longitudinal voltage V_L and obtains the resistances by $R_H = V_H/I$ and $R_L = V_L/I$.

The classical Hall resistivity gives information about both the density and the sign of charge carriers in a conductor. In fact, Hall knew that the carriers in most metals had negative charge 19 years before the electron was discovered. Hall effect measurements remain a valuable tool for characterizing samples, particularly semiconductors.

2.2 Two-Dimensional Electron Systems

The QHE takes place in a two-dimensional electron gas (2DEG), that is, a system which consists of electrons that have been dynamically confined to two dimensions. This confinement can be effected in several ways, the two most common of which are semiconductor heterostructures (such as those present in MOSFETs) and quantum wells. Since our experimental device is of the quantum well type, we will confine our discussion to quantum wells. Figure 2.2 depicts a typical quantum well. Such structures are usually grown using a technique called molecular beam epitaxy (MBE) which enables the creation of extremely high-mobility devices with properties tailored to the observation of the QHE.

A 2DEG occurs in a quantum well device because the width of the well is sufficiently small to cause the energy levels of the electrons to be quantized. If the temperature is low enough that all of the electrons are in the lowest energy level, then they will

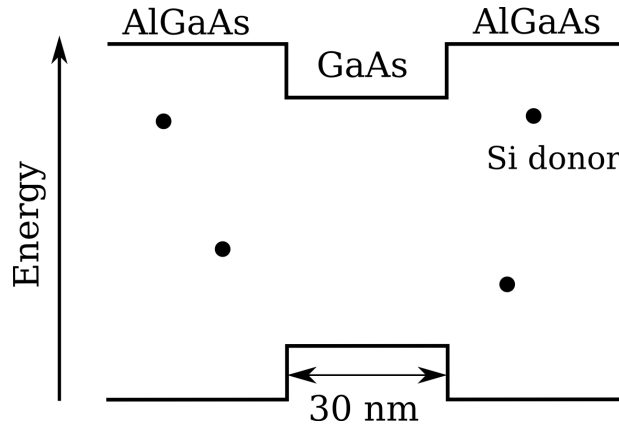


Figure 2.2: Band diagram of a GaAs-AlGaAs quantum well. The difference in band gaps between AlGaAs and GaAs creates a potential well. A 2DEG is created when the AlGaAs is doped with electrons. The donors migrate into the GaAs and fall into the potential well, thus becoming confined. The horizontal axis corresponds to the direction of deposition on the physical wafer.

no longer be free to move in the dimension corresponding to the quantum well. The electrons are still free to move in the other two spatial dimensions and hence a 2DEG is created.

2.3 Integral Quantum Hall Effect

We wrote in the introduction that the IQHE is due to two factors: the formation of LLS and disorder-induced localization. We will explore this in more depth in this section¹.

2.3.1 Landau Levels

The energy levels of electrons in a strong magnetic field are quantized. We wish to focus on the physics here, so we will simply state the result and refer the reader to the above references for a derivation. As it turns out, in our case the problem of non-relativistic charged particles in a magnetic field is equivalent to a harmonic oscillator

¹A detailed review can be found in e.g. Prange and Girvin's text [19], Girvin's notes [8], or Goerbig's notes [9].

problem. The relevant energies are

$$E_n = \hbar\omega_c \left(n + \frac{1}{2} \right) \quad (2.4)$$

where $\hbar\omega_c = \frac{e\hbar B}{m_c}$ is the cyclotron energy. The cyclotron energy defines the relevant energy scale for the Landau levels. This gives the condition that the QHE is only observed at low temperature, for we must have that $kT \ll \hbar\omega_c$ to see any effects of LLS. Each LL is massively degenerate, having $N = AB/\phi_0$ states. Here, A is the area of the sample and ϕ_0 is the magnetic flux quantum, equal to $\phi_0 = h/e$. For a typical magnetic field of perhaps 5 T and a sample with an area of 1 cm², this means that approximately 2×10^{11} electrons occupy each LL. The filling factor, ν , is defined to be the number of fully filled LLS and is given by

$$\nu = \frac{n_c \phi_0}{B}. \quad (2.5)$$

If we substitute this in to Equation (2.3), we find

$$R_H = \frac{1}{\nu} \frac{h}{e^2} \quad (2.6)$$

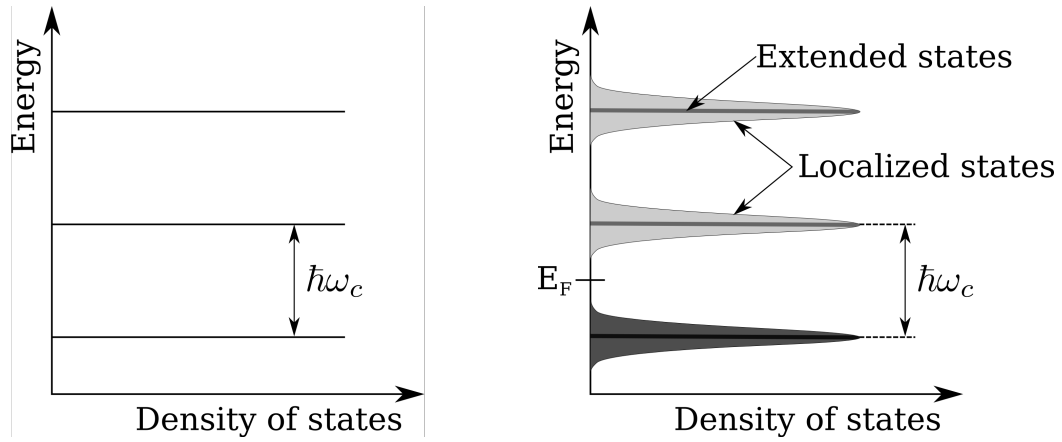
which matches Equation (1.1) for integer values of ν . However, this does not explain several of the crucial features of the IQHE. For instance, experimental IQHE traces (Figure 1.1b) show distinct plateaus around integer filling factors where the Hall resistance remains constant. Furthermore, there is the question of the observed zeros in the longitudinal resistance.

2.3.2 Localization

Localization of the electrons by weak disorder provides the necessary mechanism to explain the features of the IQHE. It is interesting to note that in a perfectly clean sample, no IQHE would be observed. The presence of disorder is essential to the formation of the IQHE state.

The effect on the LLS of introducing impurities into a clean sample can be modelled by adding an impurity potential term to Equation 2.4 to obtain

$$E_n = \hbar\omega_c \left(n + \frac{1}{2} \right) + V(\mathbf{r}) \quad (2.7)$$



(a) With no impurities, the LLS are manifest as a series of delta spikes. An energy gap of $\hbar\omega_c$ separates the levels.

(b) Impurities broaden the LLS and produce tails of localized states. The energy gap becomes a mobility gap. It takes energy to excite a localized electron to begin traversing the sample when the Fermi level sits in the gap.

Figure 2.3: LL DOS for clean (left) and dirty (right) samples.

where $r = x\hat{x} + y\hat{y} + z\hat{z}$. The LL energy now clearly varies throughout the sample. If the impurity potential is taken to be smooth and small compared to the cyclotron energy, then the effect is to broaden the discrete LL states into LL bands. This is shown schematically in Figure 2.3. The bands have a core of extended states and a tail of localized states. This is the case because a given electron will move along an equipotential contour. When an electron has an energy close to the unperturbed Landau level energy, it is able to move throughout the sample. However, electrons which fall into potential wells or end up on potential hills are unable to escape and become localized. The localized electrons are not able to move around the sample and so are not capable of carrying current.

To see how localization creates the plateaus, let us study a clean sample (no impurities) at an integer filling factor, e.g. $\nu = n$, where the Hall resistance is equal to $R_H = h/ne^2$. If we add electrons to the sample, they simply join the other electrons in the LL and begin to carry current. Now, suppose we switch on the impurity potential before adding the electrons. With impurities present, the additional electrons become localized. That is, the Hall resistance stays constant as long as the additional electrons go into the localized states. This is a plateau. At a certain point, no more localized states are available to hold the additional electrons and the extended states start to fill

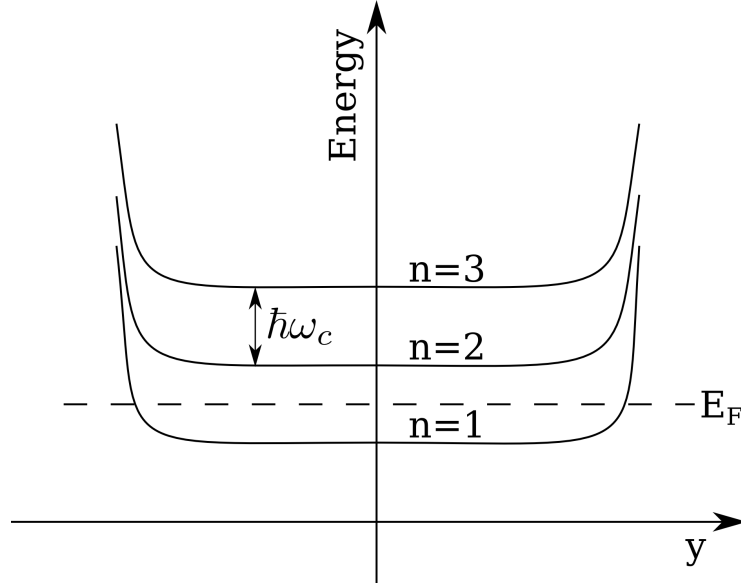


Figure 2.4: Bending of LLS as a function of transverse position y . Edge channels are formed where the Fermi level intersects upward-bent LLS.

up. As the extended states fill up, the Hall resistance decreases. When the extended states are all filled up, the Hall resistance lies in the next plateau. To summarize, when the Fermi level lies in a mobility gap (i.e. a region of localized states), the Hall resistance shows a plateau. When the Fermi level passes through the core of the LL, a transition between plateaus occurs.

2.3.3 Edge States

It is not obvious from the localization picture that that dissipationless current flow should occur (zero R_L) when the system is on a quantum Hall plateau. This experimental fact is explained by the presence of “edge states.” Edge states are one-dimensional channels running around the edge of the sample which carry current chirally (i.e. in only one direction).

Edge states arise due to the confining potential. In any physical device, the edges of the sample represent some sort of potential wall. The effect of this is to bend the LLS upwards at the edges (Figure 2.4). When the Fermi level lies in a mobility gap (i.e. when the system is on a plateau) energetic electrons which are injected at one end of the device and extracted at the other end (this corresponds to a current flowing through the device) occupy the edge states. Since the edge states are chiral, electrons

flow through the edge channels without any backscattering. Hence, an electron has a 100% probability of making it from the current injection site to the current extraction site. This means that when the system is on a plateau, the longitudinal resistance is zero.

2.4 Fractional Quantum Hall Effect

Unlike the IQHE, which is a state experienced by non-interacting electrons, the FQHE is fundamentally a phenomenon of highly correlated electrons. The physics of the FQHE cannot be deduced from considerations of LLS and disorder; it is strongly non-perturbative.

The theory of the FQHE² is a broad subject. However, there exists a particularly simple and elegant description of the phenomenology of the FQHE in terms of so-called composite fermions. A composite fermion is the bound state of an electron and an even number of quantized vortices. In the context of CF theory, a vortex is a theoretical construct represented by a zero in the complex wave function. The defining property of a vortex is that a closed path around it gives a contribution of 2π to the phase of the wave function. A vortex attached to an electron can be thought of as analogous to a single flux quantum attached to an electron. Strongly correlated electrons in a magnetic field B become composite fermions by binding themselves to vortices to screen the Coulomb repulsion between them. These composite fermions are themselves weakly interacting and experience an effective magnetic field B^* .

It turns out [12] that the FQHE is equivalent to the IQHE of composite fermions. That is, electrons at fractional filling factor ν correspond to composite fermions at integer effective filling factor ν^* . Hence, most of the phenomena of the IQHE carry over to the FQHE. This includes quantized Hall resistance at certain fractional filling factors and zero longitudinal resistance on plateaus. Importantly, the incompressibility of the IQHE states carries over to the FQHE states. The CF approach can be used to construct microscopic wave functions for the FQHE that have been shown to have excellent agreement with experiment.

²FQHE theory is well-reviewed in the previously referenced [8, 9, 19]. CF theory in particular is excellently described in Jain's text [13].

2.4.1 The $\frac{5}{2}$ State

The $\frac{5}{2}$ state, along with some other even-denominator states, is special because it is not explained by the CF theory, which can only describe odd-denominator fractions. This fact comes from the requirement that the CF wave function be antisymmetric (fermionic) under exchange. However, an incompressible state showing all the hallmarks of the FQHE does exist at $\frac{5}{2}$. As mentioned in Chapter 1, this state is believed to be a paired state of composite fermions. The state results from the fact that the interaction between composite fermions at this factor is actually weakly attractive [22]. The wave function describing the $\frac{5}{2}$ state is highly analogous to a BCS wavefunction for Cooper pairs. Importantly, this paired state is gapped and supports an FQHE at $\frac{5}{2}$. The exact form of the excitations has yet to be conclusively identified; however, for some hint of what they might look like, we refer the reader to a recent paper by Rodriguez et al. [20].

2.4.2 Thermal Activation

It is an experimental fact that the longitudinal resistance R_L associated with a quantum Hall plateau is temperature dependent [2, 3, 24]. While R_L is truly zero at zero temperature, at any finite temperature there is some activation away from zero resistance. This temperature dependence can be due to several different mechanisms, including variable-range hopping effects. However, at high temperature, it is due to thermal activation where electrons (composite fermions in the case of the FQHE) gain enough energy to be able to bridge the mobility gap and cross the sample. Empirically, R_L is described by an Arrhenius law:

$$R_L \propto \exp\left(-\frac{\Delta}{2T}\right) \quad (2.8)$$

where Δ is the gap. This thermal activation behavior gives us an experimental method which can be used to determine the gap. Measuring the temperature dependence of the minimum in R_L evidently tells us the gap energy.

Chapter 3

Experiment

3.1 Sample

For this measurement, we used a high quality GaAs-AlGaAs quantum well sample grown by Manfra¹ at a state-of-the art MBE facility. The sample had a carrier density of $3.1 \times 10^{11} \text{ cm}^{-2}$, as determined from low-field Shubnikov-de Haas oscillations.

Electrical contact to the sample was made with gold bond wires pressed to indium contacts. The sample had already been prepared with indium contacts when we received it. First, we placed the sample in a non-magnetic ceramic chip carrier and secured it with poly(methyl methacrylate) (PMMA), a polymer which we use as a removable glue. Then, using a wire bonder and small blobs of indium, we secured gold bond wires to the existing indium contacts and to the contact pads on the chip carrier.

3.2 Measurement

To cool the sample, we employed a dilution refrigerator which is capable of reaching a base temperature of approximately 12 mK. Dilution refrigerators use a thermodynamic cycle carried out in a mixture of ^3He / ^4He to produce large cooling powers. A dilution refrigerator is ideal for this type of experiment because it is capable of maintaining a stable temperature for many weeks and because it offers fine-grained control of the sample temperature.

The voltages and currents involved in QHE measurements are quite small. A typical

¹<http://www.physics.purdue.edu/mbe/>

AC bias current is on the order of 1 nA and measured voltages are often on the order of 1 μ V. Hence, lock-in detection is essential. A lock-in amplifier is able to make very sensitive measurements in a noisy environment by matching the phase of the measured signal to the phase of the input signal. The phase of the noise is random and so if the measured and input signal are in phase, the measured signal can be recovered even if the signal-to-noise ratio is quite high.

To carry out temperature dependence measurements, we apply power to the mixing chamber of the dilution refrigerator until the desired temperature is reached. We measure the temperature using a RuO₂ resistive thermometer which is mounted to the mixing chamber. By applying a bias current and measuring the resulting voltages, as shown in Figure 1.2, we are able to obtain values for R_H and R_L . We made these resistance measurements over a range of temperatures from 60 mK to 120 mK.

Chapter 4

Results and Discussion

Figure 4.1 shows a base temperature overview of the QHE in our sample in the region between $\nu = 2$ and $\nu = 4$. A strong $\frac{5}{2}$ state is visible along with other FQHE states. Figure 4.2 shows a detailed view of the minimum in R_L associated with the $\frac{5}{2}$ state. The minimum has a wide, flat bottom which tells us that the $\frac{5}{2}$ state is very well developed. There are no signs of thermal activation at this temperature.

The results of our temperature dependence measurements can be seen in Figure 4.3. The thermal activation of the $\frac{5}{2}$ state is easily seen as the minimum in R_L lifts away from zero resistance. As the temperature rises, excitations from the $\frac{5}{2}$ state gain enough thermal energy to overcome the mobility gap and conduct current through the bulk of the sample. This causes the longitudinal resistance to deviate from its zero value.

To obtain the value for the gap, we use the Arrhenius law given in Equation 2.8. We make an “Arrhenius plot” with $1/T$ as the abscissa and the natural logarithm of the minimum resistance value as the ordinate. The Arrhenius activation behavior appears as a straight line whose slope is equal to $-\Delta/2T$. By fitting to this line, we obtain a value for the gap. An Arrhenius plot of our data is shown in Figure 4.4. By fitting to the linear portion of the plot, we obtain a value for the gap of (537 ± 34) mK. We have ignored, for the purposes of fitting, the data which are not linear. This is in fact the physically correct thing to do because the Arrhenius activation behavior only holds in some region of temperatures. At lower temperature, thermal activation freezes out and hopping transport dominates [14]. At higher temperature, thermal activation saturates. Hence, Equation 2.8 is only applicable for a certain range of temperatures.

The uncertainty in our measurement is dominated by the uncertainty in the value of the minimum resistance. As can be seen in Figure 4.3, there is a certain amount of noise in the resistance data. We determine the minimum resistance by averaging over a

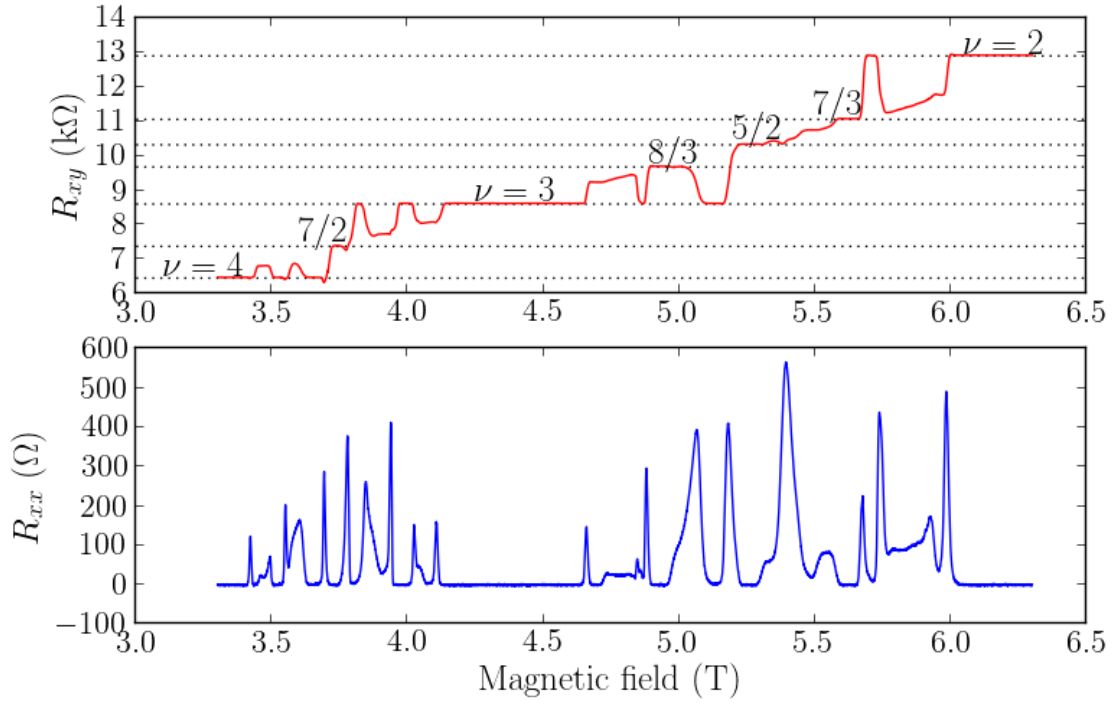


Figure 4.1: Hall and longitudinal resistances for our sample in the filling factor range from $\nu = 2$ to $\nu = 4$. Several well-developed fractional states can be seen along with a number of re-entrant integral states. These are highly interesting in their own right and are due to the formation of crystalline “bubble” and “stripe” phases. These states occur because the electron kinetic energy has frozen out and the electrons seek to minimize their Coulomb energy by forming periodic structures. The measurements shown here were made at base temperature of approximately 12 mK.

small window (15 points in our case) in the vicinity of the minimum. The uncertainty is then determined by the magnitude of the noise fluctuations divided by the square root of the number of points sampled.

To our knowledge, this gap is among the highest ever measured for the $\frac{5}{2}$ state. Previous experiments performed with high-mobility samples have found gaps in the range of approximately 200 mK to 500 mK [4, 7, 21].

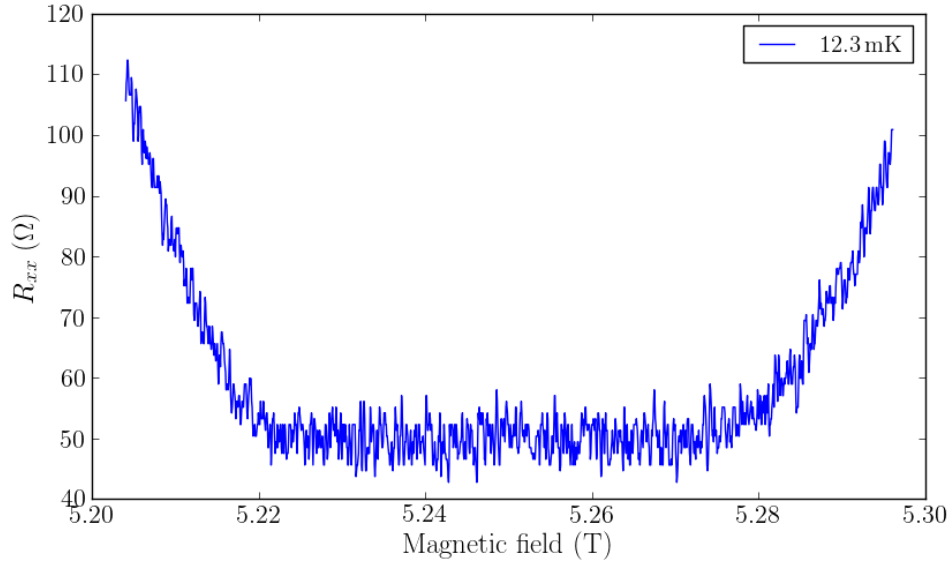


Figure 4.2: Detailed view of the $\frac{5}{2} R_L$ minimum at 12.3 mK. The nonzero value is due to frequency dependent lock-in detection problems that were later fixed.

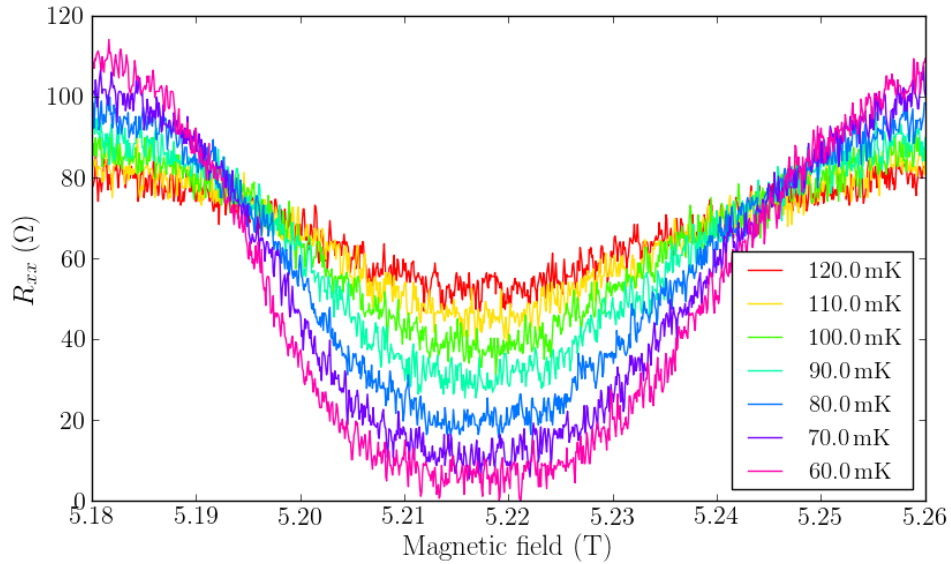


Figure 4.3: Thermal activation of the $\frac{5}{2}$ state is clearly evinced as a lifting of the minimum in R_L , which goes from nearly zero resistance to almost 60 Ω as the temperature of the sample is increased.

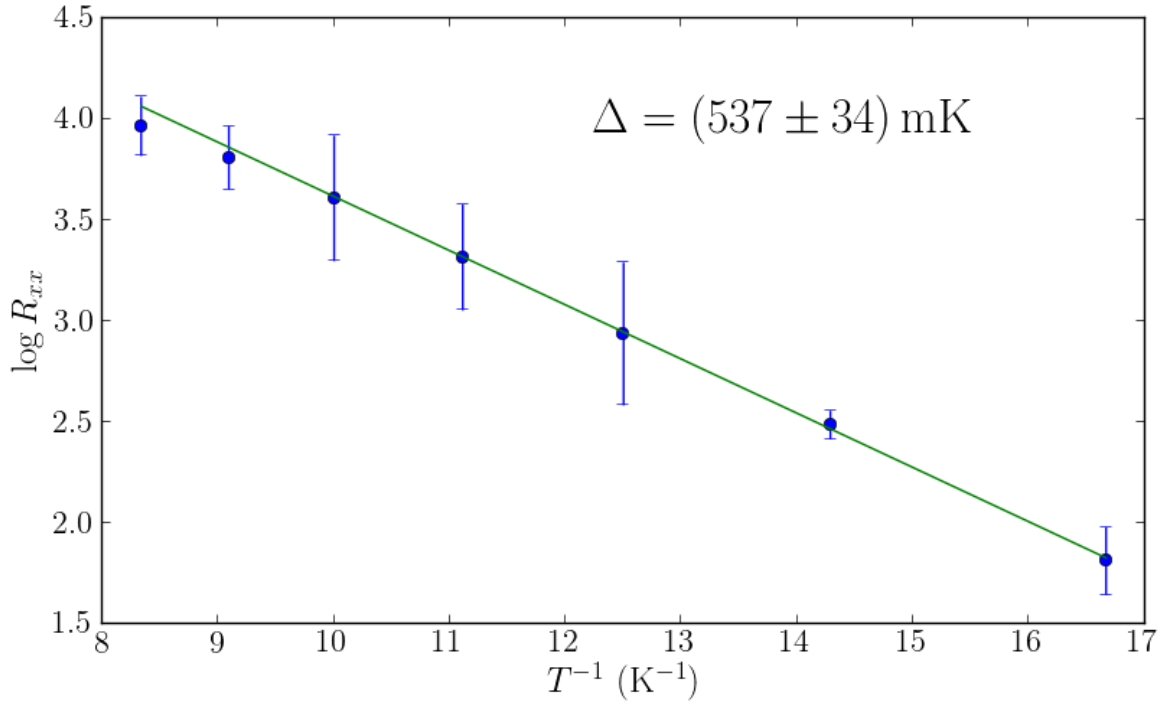


Figure 4.4: Arrhenius plot of thermal activation data. At higher temperatures (corresponding to smaller values of $1/T$), the activation saturates and no longer exhibits an Arrhenius behavior. The two highest temperature points are not included in our fit for this reason. The error bars are one standard deviation.

Chapter 5

Conclusion

We have measured the energy gap of the $\frac{5}{2}$ FQHE state in a high-mobility GaAs-AlGaAs quantum well. We used the Arrhenius behavior of the temperature dependence of the minimum in R_L to extract the gap energy. We find that $\Delta = (537 \pm 34)$ mK, which is similar to values reported by others for comparable samples.

The $\frac{5}{2}$ FQHE state is a fascinating collective state of matter where electrons bind to flux vortices to form composite fermions which then condense into “Cooper pairs.” It offers rich possibilities for future research. The exact nature of the state and its quasiparticle excitations have yet to be conclusively demonstrated and it is still an open question whether $\frac{5}{2}$ supports non-Abelian anyons. If it does, the state presents a highly promising candidate for realizing topologically protected quantum computing.

Bibliography

- [1] B. Blok and X. Wen. Many-body systems with non-abelian statistics. *Nuclear Physics B*, 374(3):615 – 646, 1992. ISSN 0550-3213. doi:10.1016/0550-3213(92)90402-W. URL <http://www.sciencedirect.com/science/article/pii/055032139290402W>.
- [2] G. S. Boebinger, A. M. Chang, H. L. Stormer, and D. C. Tsui. Magnetic field dependence of activation energies in the fractional quantum hall effect. *Phys. Rev. Lett.*, 55:1606–1609, Oct 1985. doi:10.1103/PhysRevLett.55.1606. URL <http://link.aps.org/doi/10.1103/PhysRevLett.55.1606>.
- [3] A. M. Chang, M. A. Paalanen, D. C. Tsui, H. L. Störmer, and J. C. M. Hwang. Fractional quantum hall effect at low temperatures. *Phys. Rev. B*, 28:6133–6136, Nov 1983. doi:10.1103/PhysRevB.28.6133. URL <http://link.aps.org/doi/10.1103/PhysRevB.28.6133>.
- [4] H. C. Choi, W. Kang, S. Das Sarma, L. N. Pfeiffer, and K. W. West. Activation gaps of fractional quantum hall effect in the second landau level. *Phys. Rev. B*, 77:081301, Feb 2008. doi:10.1103/PhysRevB.77.081301. URL <http://link.aps.org/doi/10.1103/PhysRevB.77.081301>.
- [5] N. R. Cooper and A. Stern. Observable bulk signatures of non-abelian quantum hall states. *Phys. Rev. Lett.*, 102:176807, Apr 2009. doi:10.1103/PhysRevLett.102.176807. URL <http://link.aps.org/doi/10.1103/PhysRevLett.102.176807>.
- [6] S. Das Sarma, M. Freedman, and C. Nayak. Topologically protected qubits from a possible non-abelian fractional quantum hall state. *Phys. Rev. Lett.*, 94:166802, Apr 2005. doi:10.1103/PhysRevLett.94.166802. URL <http://link.aps.org/doi/10.1103/PhysRevLett.94.166802>.
- [7] C. R. Dean, B. A. Piot, P. Hayden, S. Das Sarma, G. Gervais, L. N. Pfeiffer, and K. W. West. Intrinsic gap of the $\nu = \frac{5}{7}2$ fractional quantum hall state. *Phys. Rev. Lett.*, 100:146803, Apr 2008. doi:10.1103/PhysRevLett.100.146803. URL <http://link.aps.org/doi/10.1103/PhysRevLett.100.146803>.

- [8] S. M. Girvin. Course 2: The Quantum Hall Effect: Novel Excitations and Broken Symmetries. In A. Comtet, T. Jolicoeur, S. Ouvry, and F. David, editors, *Topological Aspects of Low Dimensional Systems*, page 53, 1999.
- [9] M. O. Goerbig. Quantum Hall Effects. *ArXiv e-prints*, Sept. 2009.
- [10] M. Greiter, X. Wen, and F. Wilczek. Paired hall states. *Nuclear Physics B*, 374(3): 567 – 614, 1992. ISSN 0550-3213. doi:10.1016/0550-3213(92)90401-V. URL <http://www.sciencedirect.com/science/article/pii/055032139290401V>.
- [11] E. H. Hall. On a new action of the magnet on electric currents. *American Journal of Mathematics*, 2(3):287–292, Sep. 1879. URL <http://www.jstor.org/stable/2369245>.
- [12] J. K. Jain. Composite-fermion approach for the fractional quantum hall effect. *Phys. Rev. Lett.*, 63:199–202, Jul 1989. doi:10.1103/PhysRevLett.63.199. URL <http://link.aps.org/doi/10.1103/PhysRevLett.63.199>.
- [13] J. K. Jain. *Composite Fermions*. Cambridge University Press, 2007.
- [14] S. Koch, R. J. Haug, K. von Klitzing, and K. Ploog. Variable range hopping transport in the tails of the conductivity peaks between quantum hall plateaus. *Semiconductor Science and Technology*, 10(2):209, 1995. URL <http://stacks.iop.org/0268-1242/10/i=2/a=015>.
- [15] G. Moore and N. Read. Nonabelions in the fractional quantum hall effect. *Nuclear Physics B*, 360(2&A3):362 – 396, 1991. ISSN 0550-3213. doi:10.1016/0550-3213(91)90407-O. URL <http://www.sciencedirect.com/science/article/pii/055032139190407O>.
- [16] C. Nayak, S. H. Simon, A. Stern, M. Freedman, and S. Das Sarma. Non-abelian anyons and topological quantum computation. *Rev. Mod. Phys.*, 80:1083–1159, Sep 2008. doi:10.1103/RevModPhys.80.1083. URL <http://link.aps.org/doi/10.1103/RevModPhys.80.1083>.
- [17] W. Pan, J.-S. Xia, V. Shvarts, D. E. Adams, H. L. Stormer, D. C. Tsui, L. N. Pfeiffer, K. W. Baldwin, and K. W. West. Exact quantization of the even-denominator fractional quantum hall state at $\nu = 5/2$ landau level filling factor. *Phys. Rev. Lett.*, 83:3530–3533, Oct 1999. doi:10.1103/PhysRevLett.83.3530. URL <http://link.aps.org/doi/10.1103/PhysRevLett.83.3530>.
- [18] L. Pfeiffer, K. W. West, H. L. Stormer, J. P. Eisenstein, K. W. Baldwin, D. Gershoni, and J. Spector. Formation of a high quality two-dimensional electron gas on cleaved GaAs. *Applied Physics Letters*, 56(17):1697–1699, 1990. doi:10.1063/1.103121. URL <http://link.aip.org/link/?APL/56/1697/1>.
- [19] R. Prange and S. M. Girvin. *The Quantum Hall Effect*. Springer, 1990.

- [20] I. D. Rodriguez, A. Sterdyniak, M. Hermanns, J. K. Slingerland, and N. Regnault. Quasiparticles and excitons for the Pfaffian quantum Hall state. *Phys. Rev. B*, 85(3):035128, Jan. 2012. doi:10.1103/PhysRevB.85.035128.
- [21] N. Samkharadze, J. D. Watson, G. Gardner, M. J. Manfra, L. N. Pfeiffer, K. W. West, and G. A. Csáthy. Quantitative analysis of the disorder broadening and the intrinsic gap for the $\nu = \frac{5}{2}$ fractional quantum hall state. *Phys. Rev. B*, 84:121305, Sep 2011. doi:10.1103/PhysRevB.84.121305. URL <http://link.aps.org/doi/10.1103/PhysRevB.84.121305>.
- [22] V. Scarola, K. Park, and J. Jain. Cooper instability of composite fermions. *Nature*, 406(6798):863–865, Aug 2000.
- [23] D. C. Tsui, H. L. Stormer, and A. C. Gossard. Two-dimensional magnetotransport in the extreme quantum limit. *Phys. Rev. Lett.*, 48:1559–1562, May 1982. doi:10.1103/PhysRevLett.48.1559. URL <http://link.aps.org/doi/10.1103/PhysRevLett.48.1559>.
- [24] D. C. Tsui, H. L. Störmer, J. C. M. Hwang, J. S. Brooks, and M. J. Naughton. Observation of a fractional quantum number. *Phys. Rev. B*, 28:2274–2275, Aug 1983. doi:10.1103/PhysRevB.28.2274. URL <http://link.aps.org/doi/10.1103/PhysRevB.28.2274>.
- [25] K. von Klitzing. 25 years of quantum hall effect (qhe) a personal view on the discovery, physics and applications of this quantum effect. *The Quantum Hall Effect*, pages 1–21, 2005.
- [26] K. von Klitzing, G. Dorda, and M. Pepper. New method for high-accuracy determination of the fine-structure constant based on quantized hall resistance. *Phys. Rev. Lett.*, 45:494–497, Aug 1980. doi:10.1103/PhysRevLett.45.494. URL <http://link.aps.org/doi/10.1103/PhysRevLett.45.494>.
- [27] R. Willett, J. P. Eisenstein, H. L. Störmer, D. C. Tsui, A. C. Gossard, and J. H. English. Observation of an even-denominator quantum number in the fractional quantum hall effect. *Phys. Rev. Lett.*, 59:1776–1779, Oct 1987. doi:10.1103/PhysRevLett.59.1776. URL <http://link.aps.org/doi/10.1103/PhysRevLett.59.1776>.
- [28] R. L. Willett, L. N. Pfeiffer, and K. W. West. Alternation and interchange of $e/4$ and $e/2$ period interference oscillations consistent with filling factor $5/2$ non-abelian quasiparticles. *Phys. Rev. B*, 82:205301, Nov 2010. doi:10.1103/PhysRevB.82.205301. URL <http://link.aps.org/doi/10.1103/PhysRevB.82.205301>.
- [29] J. S. Xia, W. Pan, C. L. Vicente, E. D. Adams, N. S. Sullivan, H. L. Stormer, D. C. Tsui, L. N. Pfeiffer, K. W. Baldwin, and K. W. West. Electron correlation in the

second landau level: A competition between many nearly degenerate quantum phases. *Phys. Rev. Lett.*, 93:176809, Oct 2004. doi:10.1103/PhysRevLett.93.176809. URL <http://link.aps.org/doi/10.1103/PhysRevLett.93.176809>.